

Tubular Epithelial NF- κ B Activity Regulates Ischemic AKI

Lajos Markó,^{*,†} Emilia Vigolo,[†] Christian Hinze,[†] Joon-Keun Park,[†] Giulietta Roël,[†] András Balogh,^{*,†} Mira Choi,^{*} Anne Wübken,[†] Jimmi Cording,[§] Ingolf E. Blasig,[§] Friedrich C. Luft,^{*,†} Claus Scheidereit,[†] Kai M. Schmidt-Ott,^{||} Ruth Schmidt-Ullrich,[†] and Dominik N. Müller^{*,†}

^{*}Experimental and Clinical Research Center, a joint cooperation between the Charité Medical Faculty and the Max Delbrück Center for Molecular Medicine, Berlin, Germany; [†]Max Delbrück Center for Molecular Medicine, Berlin, Germany; [‡]Hannover Medical School, Hannover, Germany; [§]Leibniz-Institut für Molekulare Pharmakologie, Berlin, Germany; and ^{||}Department of Nephrology, Charité Medical Faculty, Berlin, Germany

ABSTRACT

NF- κ B is a key regulator of innate and adaptive immunity and is implicated in the pathogenesis of AKI. The cell type-specific functions of NF- κ B in the kidney are unknown; however, the pathway serves distinct functions in immune and tissue parenchymal cells. We analyzed tubular epithelial-specific NF- κ B signaling in a mouse model of ischemia-reperfusion injury (IRI)-induced AKI. NF- κ B reporter activity and nuclear localization of phosphorylated NF- κ B subunit p65 analyses in mice revealed that IRI induced widespread NF- κ B activation in renal tubular epithelia and in interstitial cells that peaked 2–3 days after injury. To genetically antagonize tubular epithelial NF- κ B activity, we generated mice expressing the human NF- κ B super-repressor I κ B $\alpha\Delta$ N in renal proximal, distal, and collecting duct epithelial cells. Compared with control mice, these mice exhibited improved renal function, reduced tubular apoptosis, and attenuated neutrophil and macrophage infiltration after IRI-induced AKI. Furthermore, tubular NF- κ B-dependent gene expression profiles revealed temporally distinct functional gene clusters for apoptosis, chemotaxis, and morphogenesis. Primary proximal tubular cells isolated from I κ B $\alpha\Delta$ N-expressing mice and exposed to hypoxia-mimetic agent cobalt chloride exhibited less apoptosis and expressed lower levels of chemokines than cells from control mice did. Our results indicate that postischemic NF- κ B activation in renal tubular epithelia aggravates tubular injury and exacerbates a maladaptive inflammatory response.

J Am Soc Nephrol 27: 2658–2669, 2016. doi: 10.1681/ASN.2015070748

AKI is common, affects >13 million people per year worldwide, and causes about 1.7 million deaths yearly.^{1,2} Ischemia is frequently involved, and an inflammatory response to sterile cell death or injury is common.³ The transcription factor NF- κ B controls many cellular processes, including immune and inflammatory responses, cell proliferation and migration, apoptosis, and differentiation. The mammalian NF- κ B family consists of five members—p65 (RelA), c-Rel, RelB, p50/p105 (NF- κ B1), and p52/p100 (NF- κ B2)—that form various heterodimers or homodimers.⁴ In the absence of any stimuli, NF- κ B is sequestered in the cytoplasm by NF- κ B inhibitors (I κ Bs). Specific stimuli lead to phosphorylation of I κ B proteins

by the I κ B kinase complex, which results in ubiquitination and degradation of I κ Bs and subsequent

Received July 8, 2015. Accepted November 26, 2015.

L.M. and E.V. contributed equally to this work. K.M.S.O., R.S.U., and D.N.M. contributed equally as principal investigators.

Published online ahead of print. Publication date available at www.jasn.org.

Correspondence: Dr. Lajos Markó, Experimental and Clinical Research Center, Lindenberger Weg 80, 13125 Berlin, Germany, or Dr. Dominik N. Müller, Experimental and Clinical Research Center, Lindenberger Weg 80, 13125 Berlin, Germany. Email: lajosmarko@yahoo.com or dominik.mueller@mdc-berlin.de

Copyright © 2016 by the American Society of Nephrology

translocation of NF- κ B to the nucleus.^{4,5} NF- κ B binds to specific sequences in the promoter or enhancer regions of target genes, which include genes encoding proinflammatory effectors as well as of I κ B proteins to restore the steady state.⁶ The p65-p50 dimer (here referred to as NF- κ B) is the heterodimer most frequently activated by a wide range of stimuli relevant to kidney injury, including cytokines and growth factors, pathogen-associated damage, and metabolic stress.⁷

Several approaches have previously been used to elucidate the role of NF- κ B in AKI, including an NF- κ B decoy strategy in rat kidney allograft transplantation⁸ and rat renal ischemia-reperfusion injury (IRI),⁹ or systemic administration of small interfering RNAs targeting RelB¹⁰ or I κ B kinase subunit β ¹¹ in murine AKI models. However, NF- κ B was inhibited in all cell types in these models, thereby providing only limited information about cell-specific NF- κ B functions in the kidney during AKI. Previous studies in intestine and skin have highlighted the importance of distinguishing the effects of NF- κ B in immune cells and in tissue parenchymal cells.¹² Whereas NF- κ B signaling is frequently proinflammatory,^{13–15} intestinal epithelial-specific or keratinocyte-specific NF- κ B inhibition also can promote repair, indicating a substantial complexity of the cell type-specific NF- κ B functions.^{16,17}

We aimed to determine the *in vivo* time course of NF- κ B activation and its function in renal tubular epithelial cells during ischemic AKI. To assess the *in vivo* time course, we generated an NF- κ B reporter mouse model in which the luciferase gene is controlled by NF- κ B. Furthermore, a mouse model with tubule-specific NF- κ B suppression was produced. In combination with *in vitro* studies using isolated primary proximal tubular cells, we show that NF- κ B plays an important role in controlling the recruitment of proinflammatory cells and in processes leading to apoptosis after hypoxia.

RESULTS

In Vivo NF- κ B Activity After Ischemia-Induced AKI

To assess the time course of NF- κ B activation following IRI-induced AKI, we generated a transgenic mouse model expressing the luciferase gene under the control of NF- κ B (κ -Luc). A gradually increased NF- κ B activity was detected in κ -Luc mice after ischemia-induced AKI by measuring *in vivo* luciferase activity in the kidney (Figure 1A). NF- κ B activation increased significantly 12 hours after ischemia compared with findings in sham-operated mice (Figure 1B). The peak of NF- κ B activity

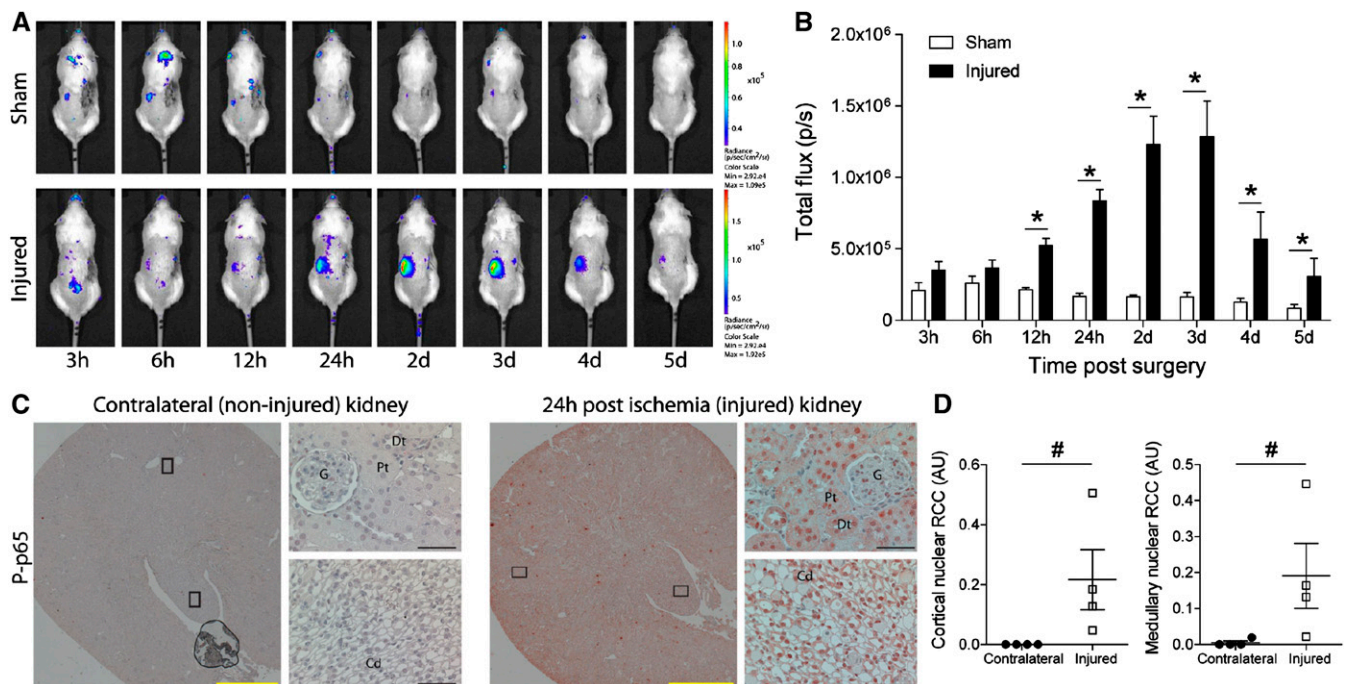


Figure 1. Time course and localization of NF- κ B activity in AKI. (A) *In vivo* bioluminescence whole-body imaging of κ -Luc mice following right uninephrectomy and sham surgery (control; upper panel) or 17.5 minutes of left renal ischemia (lower panel). After the procedure, mice were imaged at time points stated below. (B) NF- κ B-driven luciferase activity in sham-operated mice (white bars; $n=3$) and in mice with ischemic kidney injury (black bars; $n=4$). $n_{\text{Control}}=15$, $n_{\text{Emx1-}\Delta N}=15$; * $P<0.05$, Student's t test. p/s, photons/sec. (C) Immunostaining of contralateral kidney (noninjured; left panel) and of kidney 24 hours after ischemia (injured; right panel) with an antibody against phosphorylated (P) p65. Cd, collecting duct; Dt, distal tubule; G, glomeruli; Pt, proximal tubule. Black frames indicate sites of $\times 400$ magnification. Yellow bars represent 1000 μm , and black bars represent 50 μm . (D) Quantification of nuclear P-p65 staining in cortex (left panel) and medulla (right panel). RCC, red channel count (see Concise Methods). $n_{\text{Contralateral}}=4$, $n_{\text{Injured}}=4$; # $P<0.05$, Mann-Whitney U test.

was reached 2–3 days after ischemia and gradually decreased thereafter (Figure 1B). To define the cell types in which NF- κ B was activated, we stained uninephrectomized kidneys (as internal control) and kidneys after 24 hours of ischemia with an anti-phospho-S276-p65 (RelA) antibody to determine nuclear translocation of NF- κ B. In kidneys subjected to ischemic injury followed by 24 hours of reperfusion, widespread nuclear phospho-p65 staining was observed in most tubular epithelial cells, as well as in interstitial cells, whereas cells of the contralateral control kidney were not stained (Figure 1, C and D).

Generation of a Genetic Mouse Model with Tubular Epithelial-Specific NF- κ B Inhibition

To address the role of renal tubular NF- κ B signaling in ischemic AKI, we generated a mouse model with tubular epithelial-specific NF- κ B suppression using the Cre-loxP technology. First, we mated *Emx1-Cre* mice (<http://www.informatics.jax.org/allele/MGI:1928281>) with *Rosa 26 reporter* (*R26R*) mice to generate *Emx1Cre;R26R* reporter mice expressing β -galactosidase in cells

with Cre-mediated recombination.¹⁸ Immunofluorescence staining revealed β -galactosidase expression in proximal tubules labeled by aquaporin-1, in distal convoluted tubules positive for the sodium chloride symporter solute carrier family 12 member 3, and in a subset of aquaporin-2-positive collecting duct cells (Figure 2A), but not in thick ascending limbs of Henle labeled by sodium-potassium-chloride cotransporter solute carrier family 12 member 2 or in the interstitium labeled by fibronectin and fibroblast-specific protein (Supplemental Figure 1A). These data confirmed a specific activity of *Emx1-Cre* in renal tubular epithelium.

To suppress NF- κ B activity in a tissue-specific manner, we used mice in which a floxed *I κ B α* Δ N (*loxP-I κ B α* Δ N) construct is expressed under control of the ubiquitously active β -catenin (*ctnnb1*) locus (Figure 2B).¹⁹ The NF- κ B super-repressor *I κ B α* Δ N lacks the N-terminal phosphorylation and ubiquitination sites of *I κ B α* and is therefore rendered insensitive to degradation.¹⁹ Offspring of matings between *Emx1-Cre* and *loxP-I κ B α* Δ N mice bearing both the *Emx1*-driven *Cre* and one floxed *I κ B α* Δ N knock-in allele are referred

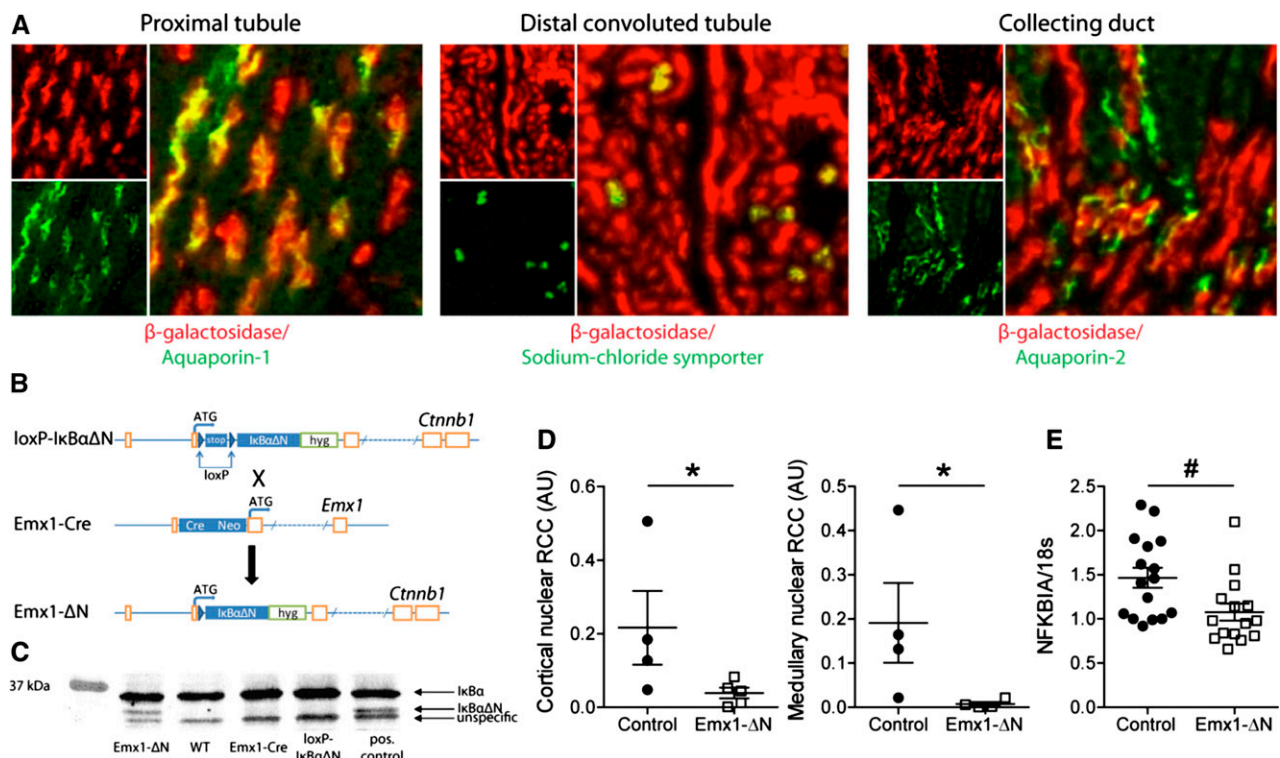


Figure 2. Generation and characterization of a mouse model with renal tubule-specific expression of the human NF- κ B super-repressor *I κ B α* Δ N. (A) Immunostaining on kidney sections from *Emx1Cre;R26R* mice using antibodies against β -galactosidase and aquaporin-1, sodium chloride symporter or aquaporin-2 to verify renal tubular Cre activity. (B) The cDNA of the NF- κ B super-repressor *I κ B α* Δ N was knocked into the β -catenin (*Ctnnb1*) locus preceded by a loxP-stop-loxP cassette (*loxP-I κ B α* Δ N). Mating of *loxP-I κ B α* Δ N with *Emx1-Cre* knockin animals generated mice expressing *I κ B α* Δ N only in cells with an active *Emx1* promoter (*Emx1- Δ N*). (C) Verification of renal *I κ B α* Δ N expression in *Emx1- Δ N* mice by Western blotting using an anti-*I κ B α* antibody. Kidney tissue lysates isolated from *I κ B α* Δ N^{ubi} mice, which constitutively express *I κ B α* Δ N ubiquitously, served as positive control. (D) Quantification of nuclear P65 staining in cortex (left panel) and medulla (right panel) from control and *Emx1- Δ N* mice 24 hours after ischemia. RCC, red channel count (see Concise Methods). $n_{\text{control}}=4$, $n_{\text{Emx1- Δ N}}=5$; * $P<0.05$, Mann-Whitney *U* test. (E) Expression of NFKBIA mRNA in control and *Emx1- Δ N* kidneys after 24-hour ischemia. $n_{\text{control}}=16$, $n_{\text{Emx1- Δ N}}=15$; # $P<0.05$, *t* test.

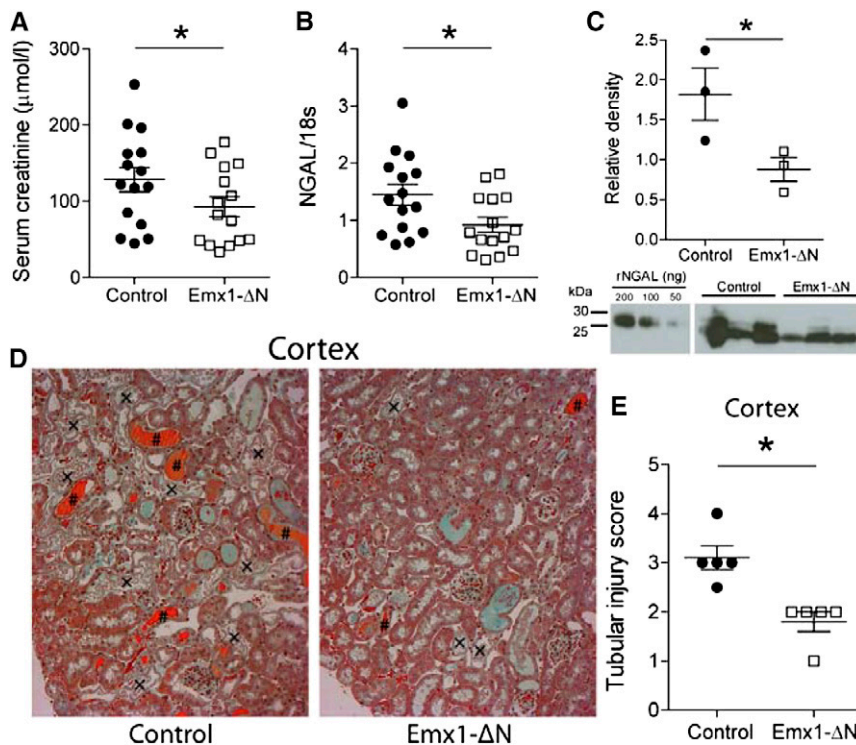


Figure 3. Suppression of NF- κ B activity in renal tubules ameliorates AKI. (A) Serum creatinine levels and (B) mRNA levels of kidney injury marker NGAL in *Emx1-ΔN* mice and control littermates 24 hours after ischemia. $n_{\text{Control}}=15$, $n_{\text{Emx1-ΔN}}=15$; * $P<0.05$, t test. (C) Urinary Western blot for analysis of NGAL expression using protein lysates from *Emx1-ΔN* mice and littermate controls. Recombinant mouse NGAL was used as a standard. $n_{\text{Control}}=3$, $n_{\text{Emx1-ΔN}}=3$; * $P<0.05$, t test. (D) Representative images of Masson trichrome stain on kidney sections of controls and *Emx1-ΔN* mice after 24 hours of ischemia (original magnification, $\times 400$). Tubular necrosis (X) and eosinophilic cellular debris (#) are shown. (E) Semiquantification of cortical tubular injury. $n_{\text{Control}}=5$, $n_{\text{Emx1-ΔN}}=5$; * $P<0.05$, t test.

to as *Emx1-ΔN* (Figure 2B). Immunoblot with $\text{I}\kappa\text{B}\alpha$ -specific antibody on kidney lysates confirmed expression of $\text{I}\kappa\text{B}\alpha\Delta\text{N}$ in *Emx1-ΔN* mice but not in controls (Figure 2C, Supplemental Figure 1B). To assess whether the tubular expression of $\text{I}\kappa\text{B}\alpha\Delta\text{N}$ reduces NF- κ B activity in the kidney after ischemic AKI, kidney sections were stained with anti-phospho-S276-p65 antibody (Supplemental Figure 1C). Twenty-four hours after ischemia, kidneys of *Emx1-ΔN* mice showed significantly less nuclear P-p65 intensity in the cortex and in the medulla compared with kidneys of control mice (Figure 2D). A detailed analysis of NF- κ B activity by P-p65 staining in the tubular nephron segments of injured control kidneys revealed a widespread nuclear P-p65 signal in segments of the nephron. In *Emx1-ΔN* mice, P-p65 signal was reduced in proximal tubules, in distal tubules, and partly in collecting ducts (Supplemental Figure 2A). Conversely, this difference was not evident in thick ascending limb of Henle loop, where Cre activity is absent (Supplemental Figure 2B). Moreover, mRNA expression of $\text{I}\kappa\text{B}\alpha$ (NFKBIA), a *bona fide* NF- κ B target gene, was significantly reduced in *Emx1-ΔN* kidneys when compared with controls (Figure 2E).

Tubular Epithelial-Specific NF- κ B Inhibition Attenuates Renal Damage after Ischemic AKI

To examine the effects of suppressed tubular NF- κ B activity on overall renal damage, we performed ischemic AKI studies in *Emx1-ΔN* and control littermates. *Emx1-ΔN* mice showed a significantly lower elevation in serum creatinine levels 24 hours after ischemia compared with control mice (Figure 3A). In addition, renal mRNA levels and urinary protein levels of the renal damage marker, neutrophil gelatinase-associated lipocalin (NGAL), were significantly lower compared with control mice (Figure 3, B and C). To assess the degree of tubular injury, kidney sections were stained and examined by an experienced renal pathologist unaware of genotype. These histologic analyses clearly indicated an amelioration of cortical tubular ischemic injury in *Emx1-ΔN* mice as they presented less tubular necrosis and less tubular lumen occluded with cellular debris in the cortex (Figure 3D). In addition, the tubular injury score showed more intense damage in control mice compared with *Emx1-ΔN* mice (Figure 3E). Additional analysis of the S3 segments of the proximal tubule, which are most susceptible to ischemic injury, showed similar differences (Supplemental Figure 3, A and B).

Reduced Apoptosis and Inflammation in *Emx1-ΔN* Mice after Ischemic AKI

AKI is associated with increased infiltration of monocytes/macrophages and neutrophils, which contribute to the proinflammatory response in early AKI.²⁰ To detect neutrophil and macrophage recruitment in the injured kidneys, we performed immunostaining and subsequently counted-labeled infiltrating cells in the outer medulla. Neutrophil and macrophage infiltration was significantly reduced 24 hours after ischemia in kidneys of *Emx1-ΔN* mice, compared with control mice (Figure 4, A–D).

Renal tubular epithelial apoptosis can initiate reperfusion-induced inflammation and subsequent tissue injury.²¹ Because NF- κ B plays an important role in apoptosis,²² we aimed to determine the number of apoptotic tubular cells in the injured kidneys of control and *Emx1-ΔN* mice. Interestingly, compared with injured kidneys of control mice, kidneys of *Emx1-ΔN* mice showed a decreased rate of apoptosis as visualized by terminal deoxynucleotidyl transferase-mediated digoxigenin-deoxyuridine nick-end labeling (TUNEL) labeling 24 hours after ischemia (Figure 5A). Quantification by direct

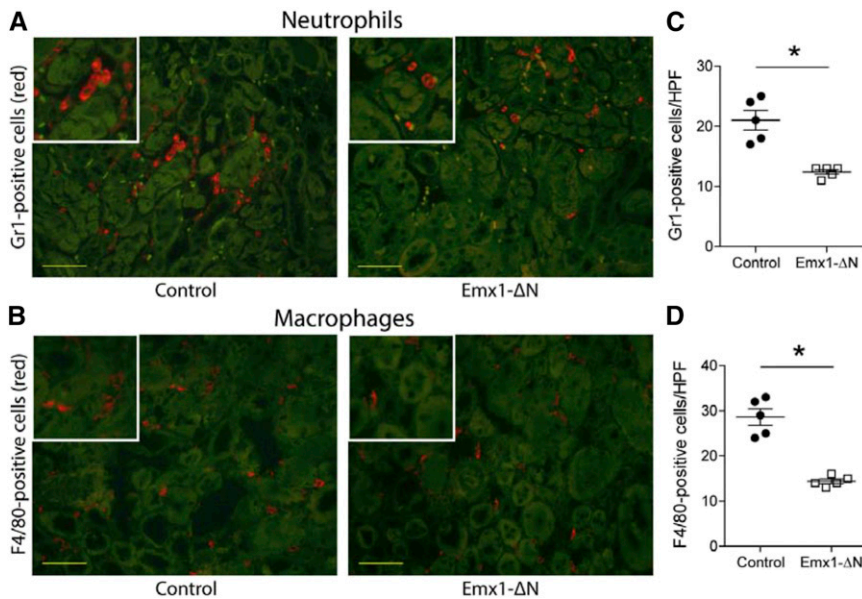


Figure 4. Inhibition of NF- κ B activity in renal tubules is associated with reduced cellular infiltration after AKI. Immunofluorescence staining for neutrophil granulocyte marker Gr1 (red [A]) and for dendritic cell/macrophage marker F4/80 (red [B]) on representative kidney sections of control and *Emx1-ΔN* mice showing the outer medulla 24 hours after ischemia. Green staining is due to autofluorescence of tubules. Yellow bars represent 50 μ m. Quantification of Gr1-positive (C) and F4/80-positive (D) cells. Each dot represents a single animal and is the mean of 20 randomly selected high-power fields (HPFs). $n_{\text{Control}}=5$, $n_{\text{Emx1-}\Delta N}=5$; * $P<0.05$, t test.

counting of TUNEL-positive tubular cells confirmed this observation (Figure 5B).

NF- κ B-Dependent Gene Signature Following Ischemic AKI

To further define the effect of reduced tubular NF- κ B signaling in the kidney following ischemic AKI, we performed microarray analysis on kidney samples, which were obtained

from *Emx1-ΔN* or control mice 24 hours after induction of ischemia. Volcano plot revealed 240 genes differentially downregulated and 250 genes differentially upregulated in kidneys of *Emx1-ΔN* mice compared with controls (fold change ≥ 1.2 and $P<0.05$) (Figure 6A). Gene-set enrichment analysis²³ confirmed a highly significant overrepresentation of known NF- κ B target genes within downregulated genes (Supplemental Figure 4A).

CD14 is a surface antigen preferentially expressed on monocytes/macrophages. The heterodimer calprotectin (S100A8/A9), which has a wide plethora of intra- and extracellular functions, colocalizes with Ly6G-positive neutrophils in AKI.²⁴ The mRNA levels of these proteins were significantly less expressed in injured kidneys of *Emx1-ΔN* mice compared with controls (Figure 6B). Moreover, gene expression of vascular cell adhesion molecule-1 (VCAM-1), as well as of the proinflammatory cytokines (IL-1 β and IL-6) and chemokines (chemokine [C-X-C motif] ligand 1 [CXCL1] and 2 [CXCL2]), were significantly reduced in injured kidneys of *Emx1-ΔN* mice compared with controls (Figure 6B).

For a more detailed investigation of the dynamics of the gene regulatory network governed by NF- κ B, we analyzed gene expression at time points 6 hours, 24 hours, 48 hours, and 7 days after IRI-induced AKI in C57Bl/6J mice. We restricted our analysis to differentially downregulated genes in *Emx1-ΔN* compared with controls because they have shown enrichment for known NF- κ B targets in gene-set enrichment analysis (Supplemental Figure 4A). Most of these genes exhibited a

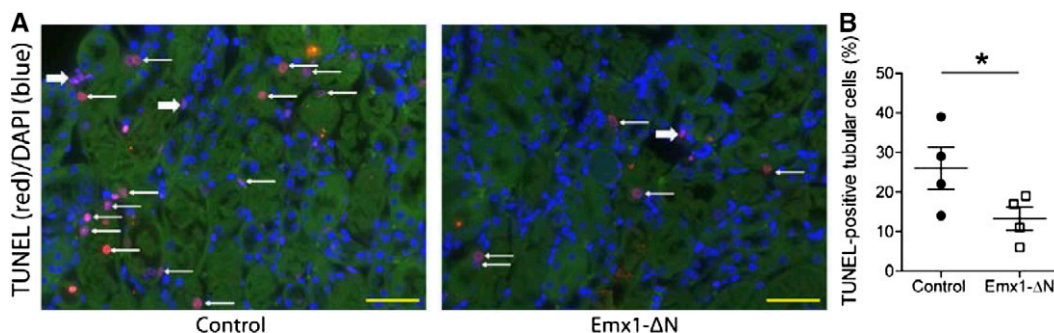


Figure 5. Inhibition of NF- κ B activity in renal tubules leads to reduced apoptosis upon AKI. (A) Representative $\times 400$ images of TUNEL labeling on control and *Emx1-ΔN* kidney sections 24 hours after renal ischemia. Thin white arrows indicate TUNEL-positive tubular cells. Thick white arrows indicate TUNEL-positive interstitial cells. Yellow bars represent 50 μ m. (B) TUNEL labeling was quantified by direct counting of the number of positively stained tubular cells, which was divided by the total number of cells per $\times 630$ field. Each dot represents a single animal and is the mean of five randomly selected outer medulla fields per animal. $n_{\text{Control}}=4$, $n_{\text{Emx1-}\Delta N}=4$; * $P<0.05$, t test.

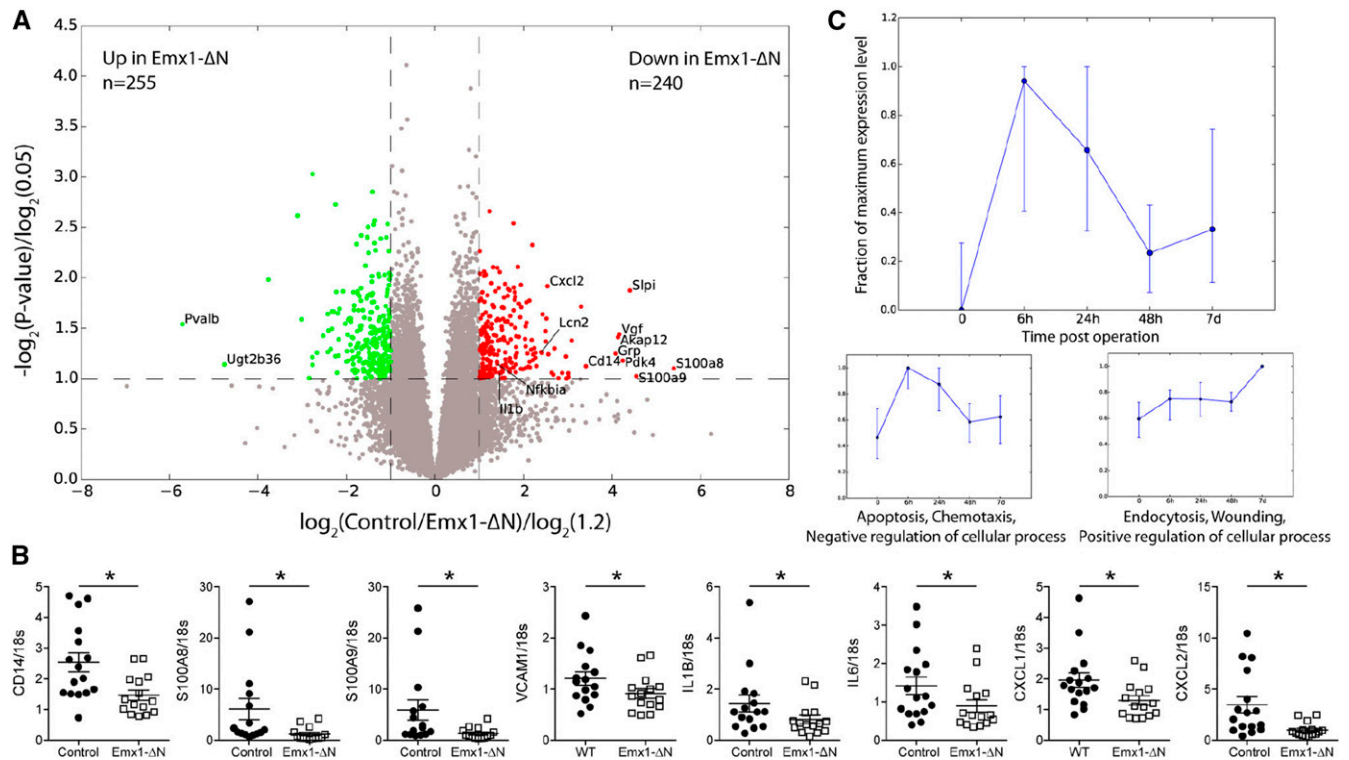


Figure 6. Microarray analysis comparing the gene expression profile of control versus *Emx1-ΔN* kidneys after ischemia. (A) Volcano plot for genes obtained from microarray analysis. Axes show logarithmic transformation of fold changes (x-axis) and *P* values (y-axis). Genes differentially expressed (fold change ≥ 1.2 and $P < 0.05$) are in green if upregulated in *Emx1-ΔN* mice compared with controls and in red if downregulated. (B) Verification by quantitative real-time PCR of some of the NF- κ B target genes downregulated in injured *Emx1-ΔN* kidneys. $n_{\text{Control}}=15$, $n_{\text{Emx1-}\Delta\text{N}}=15$; WT, wild-type. $*P < 0.05$, *t* test. (C) Time-dependent expression pattern of all genes downregulated in injured kidneys of *Emx1-ΔN* mice compared with controls (red dots in A) at 0, 6, 24, and 48 hours and 7 days after ischemia. Displayed are time points 0, 6, 24, and 48 hours and 7 days. The upper panel shows median and quartiles for all differentially expressed genes downregulated in *Emx1-ΔN* compared with control, while the lower two panels are result of k-means clustering of these genes with respect to their timewise expression pattern (see Concise Methods for details). For each cluster, the dominant gene ontology (GO) term from gene ontology analysis and representative class members is depicted (for a full list of all members of each cluster and detailed result of GO analysis, see Supplemental Tables 1 and 2). All gene expression values have been maximum normalized for each gene.

transient peak expression at 6 hours after ischemia (Figure 6C, upper panel). However, when we performed a more detailed analysis of the gene expression time courses using k-means clustering and merging of similar clusters *a posteriori*, we found distinct subsets of genes with markedly different expression patterns (see Concise Methods for a detailed description of the clustering analysis). The largest gene groups identified by this analysis comprised two gene sets, which we designated clusters 1 and 2 (Figure 6C, lower panels; see Supplemental Tables 1 and 2 for a full list of genes, clusters, and ontology terms). Cluster 1 peaked at 6 hours following AKI and quickly returned to baseline thereafter. This cluster contained genes mostly involved in apoptosis, cell death, and immune cell chemotaxis. Cluster 2 displayed a delayed expression peak at 7 days and contained genes responsible for endocytosis, immune cell apoptosis, epithelial morphogenesis, and wound healing. Hence, these findings suggest different time-dependent functions for NF- κ B signaling following ischemic AKI in the kidney. Differentially expressed genes in the NF- κ B signaling

pathway from Kyoto Encyclopedia of Genes and Genomes are shown in Supplemental Figure 4B.

NF- κ B Inhibition Leads to Reduced Apoptosis and Reduced Chemokine Expression Upon Cobalt Chloride Treatment in Primary Proximal Tubular Cells

To differentiate between direct and indirect effects of tubular NF- κ B signaling, we isolated proximal tubular epithelial cells from *IkB α ΔN^{ubi}* mice and control mice. The stabilization of hypoxia-inducible factor 1 (HIF1) α protein is a hallmark of hypoxia. To mimic hypoxia *in vitro*, cells were exposed to HIF1 α -stabilizing agent cobalt chloride (CoCl_2) in a low-glucose medium for 24 hours. We subsequently determined the percentage of apoptotic cells using Hoechst staining followed by fluorescent microscopy analyses (Figure 7A). Tubular cells expressing the NF- κ B super-repressor *IkB α ΔN* showed reduced apoptosis compared with control cells (Figure 7B). The mRNA expression of the HIF1 α target gene vascular endothelial growth factor was upregulated by CoCl_2 treatment in both groups

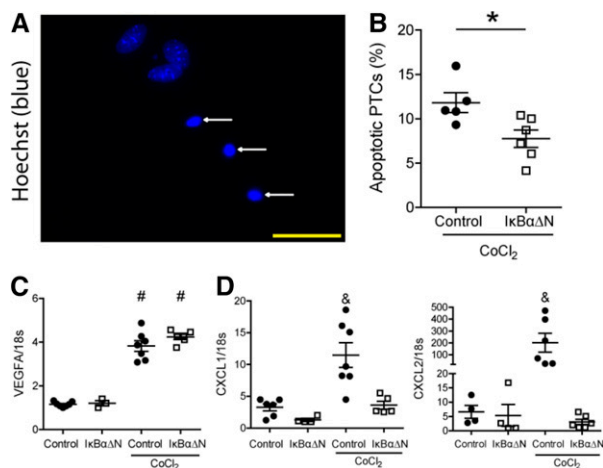


Figure 7. Primary proximal tubular cells (PTCs) overexpressing $I\kappa B\alpha\Delta N$ show less apoptosis and reduced chemotactic cytokine expression after $CoCl_2$ treatment. (A) Representative image of apoptotic PTCs (white arrows; original magnification, $\times 630$). Yellow bar represents $50\ \mu m$. (B) Quantification of apoptotic PTCs after 24-hour treatment of $300\ \mu M$ hypoxia-mimetic agent $CoCl_2$. Data are from two independent experiments. $n_{Control}=5$, $n_{I\kappa B\alpha\Delta N}=6$; $*P<0.05$, t test. mRNA expression of (C) HIF1 α target gene VEGFA and (D) chemokines CXCL1 and CXCL2. Each dot represents a pool of PTCs isolated from two to three animals of the same genotype. Data are from two independent experiments. $n_{Control}=6$, $n_{I\kappa B\alpha\Delta N}=4$, $n_{Control+CoCl_2}=7$, and $n_{I\kappa B\alpha\Delta N+CoCl_2}=6$; $\#P<0.05$ versus wild-type and $I\kappa B\alpha\Delta N$; and $P<0.05$ versus wild-type, $I\kappa B\alpha\Delta N$, and $I\kappa B\alpha\Delta N+CoCl_2$. One-way ANOVA, Newman-Keuls multiple comparison *post hoc* test.

(Figure 7C). CXCL1 and CXCL2 were induced only in control proximal tubular cells after $CoCl_2$ treatment but not in cells expressing $I\kappa B\alpha\Delta N$ (Figure 7D). Together, these data support a direct role of NF- κB signaling in tubular epithelial apoptosis and in the control of chemotactic cytokine expression by proximal tubules upon HIF1 α stabilization.

DISCUSSION

We demonstrate that inhibiting NF- κB signaling in renal tubular epithelium reduces tubular injury, apoptosis, necrosis, and accumulation of interstitial inflammatory cells, which consequently results in ameliorated kidney damage after ischemic AKI induction. The treatment of primary proximal tubular cell cultures with hypoxia-mimetic agent $CoCl_2$ further confirmed that reduced NF- κB activity *per se* reduces apoptosis and expression of certain chemokines. Previous work already implicated endothelial cell-specific suppression of NF- κB activity in the attenuation of hypertension-induced renal damage despite high BP.²⁵ Although endothelial NF- κB inhibition did not affect the development of hypertension, it diminished the upregulation of several proinflammatory NF- κB target genes, including VCAM-1 and intercellular adhesion

molecule 1 and reduced renal inflammation and tubular damage. This state of affairs suggests that renal damage is, at least in part, dependent on NF- κB activity in vascular endothelial and tubular epithelial cells. NF- κB activity in these two compartments may be required for production of cytokines and chemokines and recruitment of immune cells.

For the present study, we generated mice with suppressed NF- κB activity in the tubular epithelium ($Emx1-\Delta N$). To analyze the time course of NF- κB activation during ischemic AKI, for the first time we used a luciferase-dependent *in vivo* imaging technique using an NF- κB reporter mouse model ($\kappa-Luc$). Twelve hours after ischemic AKI induction, $\kappa-Luc$ mice revealed a significant increase of NF- κB activity, which lasted 5 days before it returned to base levels. Unfortunately, this technique does not allow us to differentiate between NF- κB activity derived from kidney cells or from infiltrating immune cells. However, phospho-p65 immunostaining showed an almost global increase of nuclear NF- κB activity in all renal compartments 24 hours following ischemic AKI induction, which suggests that a considerable amount, if not the majority, of NF- κB -induced luciferase activity stems from kidney cells.

Consistent with previous studies using global NF- κB silencing in different AKI models by injecting p105 or RelB silencing RNAs into the tail vein,^{10,26} or by injecting NF- κB decoy oligodeoxynucleotides directly into the renal artery,^{8,9,11} we also observed reduced infiltration of neutrophils and macrophages in the injured kidneys of $Emx1-\Delta N$ mice. Neutrophils and monocytes/macrophages respond rapidly to renal injury and play an important role in the deterioration of renal functions in AKI.²⁷ However, the role of different macrophage subtypes in AKI and in subsequent repair and regeneration is currently explored.²⁸ In our AKI model, the mRNA levels of a classically activated macrophage marker, inducible nitric oxide synthase, and alternatively activated macrophage marker, interferon regulatory factor 4, were not significantly reduced in injured kidneys of mice with tubular $I\kappa B\alpha\Delta N$ expression (data not shown).

Surprisingly, after ischemia we found less apoptosis in $Emx1-\Delta N$ mice compared with control mice. Although NF- κB is generally regarded as anti-apoptotic, in particular contexts and especially in response to cellular stress NF- κB can promote apoptosis.²⁹ In line with this explanation, in proximal tubular cell cultures overexpressing $I\kappa B\alpha\Delta N$ we found reduced apoptosis following hypoxia-mimetic $CoCl_2$ treatment. Nevertheless, these results should be interpreted with caution. $CoCl_2$ does not induce hypoxia but instead activates hypoxia-mediated signaling pathways under normoxia by stabilizing the cytosolic HIF1 α . Despite the proapoptotic effect of $CoCl_2$ in our model, HIF1 α can also exert antiapoptotic effects³⁰ and thus it may interfere with potential antiapoptotic effects of NF- κB suppression. Complicating issues, $I\kappa B\alpha$ has been reported to be a target of the HIF1 α -regulating hydroxylase factor inhibiting HIF.³¹ Despite these caveats, the finding of reduced apoptosis in isolated proximal tubular cells overexpressing $I\kappa B\alpha\Delta N$ suggests that the reduced apoptosis rate

represents a cell-autonomous effect of suppressed tubular NF- κ B activity in renal tubules, which is independent from the tissue microenvironment and from inflammatory cell infiltrates. Inhibition of apoptosis induced by ischemia-reperfusion was previously shown to prevent inflammation.²¹ Therefore, the reduced apoptosis observed in *Emx1- Δ N* may also contribute to the reduced immune cell infiltration seen in these mice after ischemia.

NF- κ B regulates the expression of numerous genes, including cytokines/chemokines, cell adhesion molecules and stress response genes (<http://www.bu.edu/nf-kb/>). In the context of ischemic renal injury, several NF- κ B-dependent target genes were also expressed in tubular cells.^{27,32} Indeed, following induction of ischemic AKI kidneys of *Emx1- Δ N* mice showed significantly reduced expression of the murine homologs of human IL-8, CXCL1 and CXCL2, and IL-1 β compared with control mice, which was verified in an *in vitro* model of chemical hypoxia in *I κ B α Δ N*-overexpressing primary proximal tubular cell cultures. This state of affairs indicates that tubular cells upregulate these molecules during ischemia and that their expression is dependent on NF- κ B activity. A functional role for CXCL1 and 2 in AKI was further confirmed by a study demonstrating that treatment with an inhibitor of the CXCL1/CXCL2 receptor or with neutralizing antibodies against CXCL1 or CXCL2 during renal ischemia blocked interstitial neutrophil infiltration, reduced renal damage, and improved survival.^{33,34} In addition, expression of VCAM1, which is induced on vascular endothelial cells by cytokine,³⁵ was also significantly reduced in AKI-injured *Emx1- Δ N* kidneys, suggesting a crosstalk between tubular and endothelial cells. Supporting this notion, in the study by Henke and colleagues in which NF- κ B was endothelial cell-specifically inhibited, tubular epithelial damage was also ameliorated.²⁵

Interestingly, a more detailed time course-dependent comparison of differentially expressed genes between *Emx1- Δ N* and control kidneys revealed sets of genes, which could be assigned to distinct time-dependent functions. We show here that NF- κ B is involved in regulating functional target gene programs, including cell death, which peaks approximately 6 hours after AKI induction, while repair and morphogenesis pathways peak 7 days after ischemia. In summary, this finding suggests that persistent NF- κ B activity results in time-dependent physiologic changes in the kidney, which plays an important role in the development of AKI.

NF- κ B was initially identified as a transcription factor bound to the enhancer of the immunoglobulin κ light chain gene in B lymphocytes.³⁶ The omnipotence of NF- κ B soon became clear, and many renal diseases have also been associated with impaired NF- κ B activity.^{7,37} Nevertheless, most of the evidence that links NF- κ B activation to human and experimental kidney disease is descriptive, based on experiments with cell lines or performed in a way in which the effects of NF- κ B modulation cannot be attributed to specific kidney cell types, which makes the physiologic understanding of NF- κ B in renal diseases difficult. Here we analyzed a mouse model

with specific NF- κ B suppression in the tubular epithelium. Using this mouse model we shed light on the importance of the tubular epithelium in the development of ischemic AKI. Our results may also help to improve the understanding of the role of tubular NF- κ B signaling in other renal diseases and to develop novel targeted drug treatments.

CONCISE METHODS

Mice

Transgenic mice expressing the luciferase gene under the control of NF- κ B (κ -*Luc*, *B6-Tg[κ -Luc]1Gr/Rsu*) carry 3 NF- κ B DNA-binding elements from the Ig κ light chain enhancer hooked to the luciferase gene. The luciferase reporter mice were generated on the basis of the κ -Gal construct published earlier³⁸ to noninvasively determine the *in vivo* pattern of NF- κ B activity after induction of ischemia. Albino C57BL/6 mice were used to avoid quenching of luminescence.

Mice with tubular cell-restricted NF- κ B suppression were generated by mating *Emx1-Cre* knock-in mice (*Emx1*^{tm1.1[cr]/It0}), a generous gift from Shigeyoshi Itohara, RIKEN Brain Science Institute, Hiroshima, Wako, Japan) with *floxed I κ B α Δ N* (*loxP-I κ B α Δ N*, *B6.129P2-ctnnb1*^{tm[NFKBIA Δ Nfl/f]}Rsu) mice in which the cDNA of the human NF- κ B super-repressor *I κ B α Δ N* was knocked into the β -catenin (*Ctnnb1*) locus (Figure 2A).¹⁹ Offspring that did not express *I κ B α Δ N* (wild-type, *Emx1-Cre*, or *loxP-I κ B α Δ N* mice) were used as controls. *Emx1- Δ N* mice developed normally, without any obvious phenotype. Kidneys of mice ubiquitously expressing the human NF- κ B super-repressor *I κ B α Δ N* (*I κ B α Δ N*^{ubi}; *B6.129P2-ctnnb1*^{tm[NFKBIA Δ N]1Rsu}) were used as positive control for Western blot analysis and for *in vitro* studies.¹⁹ Basal serum and urine parameters of *Emx1- Δ N* and littermate control mice are shown in Supplemental Table 3.

Emx1 promoter activity in the kidney was assessed by mating *Emx1-Cre* knockin mice with Rosa 26 reporter (*R26R*, *B6.129S-Gtosa26*^{tm1Sor}) mice.¹⁸ *Emx1-Cre*-mediated activation of β -galactosidase in the various kidney compartments was determined by using specific anti- β -galactosidase antibodies (detailed in the later section on immunofluorescence).

The Berlin Animal Review Board approved all protocols, which were conducted according to National Institutes of Health Guide for the Care and Use of Laboratory Animals standards.

In Vivo Renal Ischemia-Reperfusion Model

Male mice age 12–15 weeks were used. Anesthesia was performed with isoflurane (2.3%) in air (350 ml/min). Each mouse was operated on separately to ensure similar exposure to isoflurane (mean \pm SD, 33 \pm 3 minutes). A temperature controller with heating pad (TCAT-2, Physitemp Instruments) was used to keep body temperature stable at 37°C during surgery in order to induce warm ischemia. Rectal body temperature was continuously monitored using a sensor based on thermistors, and values were recorded at different time points. Ischemia was induced after right-sided uninephrectomy by clipping the pedicles of the remaining left kidney for 17.5 minutes with a non-traumatic aneurysm clip (FE690K, Aesculap). Reperfusion was

confirmed visually. After surgery, mice had free access to water and chow. We applied body-warm sterile physiologic saline solution and analgesia with tramadol (1 mg/kg) for every mouse. Sham surgery was performed in a similar manner, except for clamping of the renal vessels. Mice with bleeding after uninephrectomy, with incomplete renal reperfusion after ischemia, with excessive exposure of isoflurane of any reason, with significant temperature fluctuation during ischemia, or with signs for infection after 24 hours were immediately euthanized and were not used for further analysis. After 24 hours of reperfusion, mice were euthanized, and kidney and blood were collected for further analysis. The kidneys were divided into three sections. One third of the kidney was placed in optimum cutting temperature compound for immunohistochemistry, one third was immersed in 4% PBS-buffered formalin for histology, and the rest was snap-frozen in liquid nitrogen for quantitative real-time PCR.

***In Vivo* Bioluminescence Imaging of NF- κ B Activity during Reperfusion**

Two days before bioluminescence imaging, mice were shaved dorsally at the sites of the kidneys to prevent any quenching of the bioluminescent signal by the fur. κ -Luc reporter mice were anesthetized with 2.5% isoflurane and injected subcutaneously with 1.5 mg D-luciferin (VivoGlo, Promega) in 100 μ l PBS (pH, 7.0). Whole-body image was acquired after an exposure time of 60 seconds using an *In Vivo* Imaging System (IVIS Spectrum, PerkinElmer, Waltham, MA). Mice were measured at different time points after ischemia, as depicted in Figure 1A. To obtain the luciferin kinetics, every 2 minutes an image was acquired subsequently 10 times after D-luciferin injection. From the luciferin kinetics, the measurements showing maximal radiance were used for quantification. Using Living Image software, version 4.2 (Caliper LifeSciences), the bioluminescent signal was quantified. Data are presented in physical units of radiance in photons/sec per cm² per steradian.

Serum and Urine Measurements

Blood samples were taken from the left ventricle at termination. After clotting on room temperature for at least 15 minutes, blood was centrifuged at 2000 g for 10 minutes to obtain serum. Automated techniques were used to measure serum creatinine (Beckman Analyzer, Beckman Instruments). To assess basal laboratory parameters, 100 μ l blood was taken from facial region and parameters were measured using an i-STAT system with Chem8+ cartridges (Abbott Laboratories, Alameda, CA). Urine sodium and creatinine were measured in 24-hour collected urine by Labor 28 (Berlin, Germany). Urine osmolality of 24-hour collected urine was measured using freezing point depression (Advance Instruments).

Quantitative Real-Time PCR

Total RNA from snap-frozen kidneys and proximal tubular cells was isolated using RNeasy RNA isolation kit (Qiagen, Germantown, MD). RNA concentration and quality was measured by NanoDrop-1000 spectrophotometer (Thermo Fisher Scientific, Vernon Hills, IL). Two micrograms of RNA were used for cDNA transcription (Applied Biosystems, Foster City, CA). Quantitative analysis of target mRNA expression was performed with quantitative real-time PCR using the

relative standard curve method. TaqMan and SYBR green analysis was conducted using an Applied Biosystems 7500 Sequence Detector. The expression levels were normalized to 18s. Biotez synthesized the primers; the sequences are provided in Supplemental Table 4).

Microarray and K-Means Clustering

Total RNA isolated from kidneys, as mentioned before, was used for synthesis of cRNA by Illumina TotalPrep RNA Amplification kit (#AMIL1791, Thermo Fisher Scientific). The Illumina platform MouseWG-6 v2.0 Expression BeadChip Kit was used, which assays >45,000 transcripts. Kits were used according to manufacturer's instruction.

K-means clustering has been performed on the normalized gene expression data over time. That is, for each gene, we had five expression values corresponding to 0, 6, 24, and 48 hours and 7 days. These values were normalized for each single gene such that the maximum over time corresponded to 1 and the minimum to 0. These operations were performed for all genes separately. The normalized expression vectors were then clustered using k-means. For a k value of 20, 80% of the data's variance over time could be explained; thus, this k was chosen for clustering. The strongest clusters were then more closely investigated and were merged if they exhibited similar patterns over time. These analyses gave three main clusters (Figure 6C, lower panels).

Western Blot

Kidney tissues were harvested from mice with different genotypes and were lysed with RIPA buffer (Sigma-Aldrich, St. Louis, MO) supplemented with Complete Mini protease inhibitor (Roche, Basel, Switzerland) and 1 mM phenylmethylsulfonyl fluoride, phosphatase inhibitor cocktail 3 (Sigma-Aldrich) and were homogenized using a Precellys 24 homogenizator (PqLab, Erlangen, Germany). Fifty-microgram protein samples were separated by 12% SDS-PAGE. After semi-dry transfer, nonspecific binding sites of the nitrocellulose membrane were blocked with 5% nonfat milk in Tris-buffered saline containing 0.1% Tween. After that, the membrane was incubated with the primary antibody against I κ B α (1:200; sc-371 C-21, Santa Cruz Biotechnology, Santa Cruz, CA). Secondary antibody was from LI-COR Biosciences (anti-rabbit; 1:5000). Images were acquired by Odyssey infrared imaging system (LI-COR Biosciences, Lincoln, NE).

Urine was collected from the bladder of mice subjected to ischemia 24 hours following surgery. Ten microliters of urine was mixed with 4 \times nonreducing Nu-Page loading buffer (Invitrogen, Carlsbad, CA) and loaded on NuPage 4%–12% Bis-Tris gel (Invitrogen). Afterward, the proteins were blotted on a polyvinylidene fluoride membrane, which was further blocked in 5% nonfat milk in Tris-buffered saline containing 0.1% Tween for 1 hour at room temperature and then incubated overnight at 4°C with polyclonal anti-NGAL primary antibody (1:2000; #AF-1857, R&D Systems, Minneapolis, MN). Urinary NGAL was detected with horseradish peroxidase-conjugated secondary antibody (1:5000; #705-035-147, Jackson ImmunoResearch Laboratories, West Grove, PA) and chemiluminescent reagent (Super Signal-West Pico, Thermo Fisher Scientific). Known amounts of recombinant mouse NGAL protein (#1857-LC, R&D Systems) were used as standards.

Microscopy

Histology

Formalin-fixed, paraffin-embedded, 2- μ m-thick kidney sections were stained with Masson trichrome using standard protocols. The severity of tubular injury was assessed by a renal pathologist blinded to the genotype of the mice. Tubular necrosis was evaluated in a semiquantitative manner by determining the percentage of tubules in the cortex in which epithelial necrosis, loss of the brush border, cast formation, and tubular dilation were observed. A five-point scale was used: 0, normal kidney; 1, 1%–25% tubular necrosis; 2, 25%–50% tubular necrosis; 3, 50%–75% tubular necrosis; and 4, 75%–100% tubular necrosis.

Immunohistochemistry

Formalin-fixed, paraffin-embedded, 2- μ m-thick sections were stained for S276-specific phosphorylated P-p65 (1:200; ab106129, Abcam, Inc., Cambridge, MA). For visualization, the EnVision+ Kit (Dako) was used according to manufacturer's instruction; hematoxylin was used as a counterstain.

Immunofluorescence

For R26R mice, 14- μ m-thick cryosections (all other cases, 5- μ m-thick) were postfixed in ice-cold acetone, air-dried, rehydrated, and blocked with 10% normal donkey serum (Jackson ImmunoResearch Laboratories) for 30 minutes. Sections were then incubated overnight at 4°C with the following primary antibodies: rat anti-F4/80 (1:200; MCA497, AbD Serotec), rat anti-Ly-6B.2 (Gr1) (1:300; MCA771G, AbD Serotec), rabbit anti-aquaporin-1 (1:300; AB2219, EMD Millipore, Billerica, MA), rabbit anti-sodium chloride symporter (1:500; AB3553, EMD Millipore), rabbit anti-aquaporin-2 (1:500; ab15116, Abcam, Inc.), goat anti-aquaporin-2 (1:200; sc-9882, Santa Cruz Biotechnology), mouse anti-FSP (1:250; F4771, Sigma-Aldrich), rabbit anti-fibronectin (1:500; F3648, Sigma-Aldrich), rabbit anti-sodium-potassium-chloride cotransporter 2 (1:1000; gift from Sebastian Bachmann, Charité Berlin, Germany), chicken anti- β -galactosidase (1:50; ab9361, Abcam, Inc.) and rabbit anti-S276 P-p65 (1:200; ab106129, Abcam, Inc.). All incubations were performed in a humid chamber. For fluorescence visualization of bound primary antibodies, sections were further incubated with appropriate Cy3-conjugated or Alexa 488-conjugated secondary antibodies (1:500; Jackson ImmunoResearch Laboratories) for 1 hour in a humid chamber at room temperature.

TUNEL Assay

Formalin-fixed, paraffin-embedded, 2- μ m-thick sections were labeled after pepsin treatment with TMR In Situ Cell Death Detection Kit (Roche) according to the instructions of the manufacturer. Slides were counterstained with the nuclear dye 4',6-diamidino-2-phenylindole (Sigma-Aldrich) to visualize cell nuclei. Percentage of TUNEL-positive tubular cells was determined in the outer medulla by Zeiss Axio Imager. M2 fluorescence upright microscope using 63 \times Plan-Apochromat immersion oil objective (Carl Zeiss GmbH, Jena, Germany).

Apoptosis Assay

Apoptosis assay was performed as described previously.³⁹ Briefly, primary proximal tubular cells were plated onto poly-L-lysine-coated

glass coverslips and were cultured overnight. Twenty-four hours later, the medium was exchanged to fresh DMEM (Sigma-Aldrich) containing 1000 mg/L glucose, 10% FCS (Biochrom) 10%, 100 IU/ml penicillin (Sigma-Aldrich), and 100 μ g/ml streptomycin (Sigma-Aldrich). Cells were treated with 300 μ M CoCl₂ (Sigma-Aldrich) or kept untreated as described under the following section on HIF1 α stabilization in primary proximal tubular cells. After 24 hours, cells were fixed with 4% paraformaldehyde-containing PBS. Cell nuclei were stained with Hoechst 33342 fluorescent DNA dye. Nuclear morphology of the samples was scored. At least 100–150 cell nuclei per sample were analyzed on randomly chosen view fields according to typical apoptotic nuclear morphology by Zeiss Axio Imager.M2 fluorescence upright microscope using \times 63 Plan-Apochromat immersion oil objective (Carl Zeiss GmbH).

Quantitative Digital Image Analyses

All images were taken using a Zeiss Axioplan-2 imaging microscope with the computer program AxioVision 4.8 (Carl Zeiss GmbH). Intensity of the staining of P-p65 was calculated as follows: for each analyzed picture, 10 randomly chosen nuclei were cut out manually, the rest of the image was deleted. Every pixel was then transformed into an RGB (red, green, blue) number triplet and normalized to length 1 as we did not wish to measure brightness. The red channel count (RCC), as presented in the figures, is the value derived by # (pixels with entry >0.699 of the red channel in RGB after normalization)/# (pixels in the cut image). The threshold was derived from pixels of clear P-p65 staining, and the RCC is independent of image resolution. F4/80-positive and Gr1-positive cells were counted in 20 nonoverlapping view fields in the cortex and the outer medulla at \times 630 magnification. TUNEL-positive epithelial cells were counted at \times 630 magnification in five nonoverlapping outer medulla view fields, and the numbers of positive cells were divided by the total cell number of that view field.

Primary Proximal Tubular Cell Isolation

Cells were obtained and cultured as described previously.⁴⁰ Briefly, kidneys of *IkBa Δ N^{ubi}* and littermate control mice aged 10–12 weeks were euthanized by overdose of isoflurane and flushed with 10 ml ice-cold PBS (Sigma-Aldrich) through the left ventricle. Renal cortices were dissected visually and minced into small pieces. The fragments were transferred through two layers of stainless steel sieves (pore size, 125 μ m and 106 μ m; Linker). Tubular fragments caught by the 106- μ m sieve were flushed in the reverse direction with PBS and centrifuged for 5 minutes at 170 g, washed, and then resuspended into the appropriate amount of culture medium: 1:1 DMEM/F12 (D 8437; Sigma-Aldrich) supplemented with FCS 10%, penicillin 100 IU/ml, and streptomycin 100 μ g/ml buffered to a pH of 7.4. The plate was incubated in a standard humidified incubator equipped with 5% CO₂. Medium was changed 2 days later and maintained every other day until the monolayer of cells reached 90% confluence; at this time >90% of the isolated cells were megalin positive (sheep anti-LRP2 antibody [1:10,000] was a gift from Professor Thomas Willnow; secondary antibody was donkey anti-sheep Alexa 555 [1:2000; Thermo Fisher Scientific]).

HIF1 α Stabilization in Primary Proximal Tubular Cells

Primary proximal tubular cells isolated from *IkB α Δ N^{ubi}* and littermate control mice were treated with 300 μ M CoCl₂ or left untreated in a low-glucose DMEM medium (D6046, Sigma-Aldrich) for 24 hours to stabilize HIF1 α . Low-glucose medium was used because it is known that cell death in proximal tubular cell cultures is HIF1 α dependent only when glucose availability is limited.⁴¹ Optimal concentration of CoCl₂ and length of treatment were determined by preliminary experiments. After 24 hours, medium was removed and cells were harvested for further analysis.

Statistical Analyses

Statistical analyses were performed using GraphPad 5.04 (GraphPad Software, La Jolla, CA) and SPSS 13.0 (IBM SPSS, Inc., Chicago) software. Normality of the data were tested by Kolmogorov–Smirnov test. To test the presence of an outlier, the Grubbs test was used. Mann–Whitney *U* test (data with non-normal distribution) or unpaired *t* test (data with normal distribution) was used in case of two groups, as stated in figure legends. In case of more than two groups, data were analyzed by one-way ANOVA using a Newman–Keuls *post hoc* test. Data are presented as mean \pm SEM. *P* values <0.05 were considered to represent statistically significant differences.

ACKNOWLEDGMENTS

We thank Gabriele N'diaye, Dr. Sabine Bartel, May-Britt Köhler, Sarah Ugowski, and Petra Berkefeld for their excellent technical assistance.

This work was supported by the Deutsche Forschungsgemeinschaft (DFG) (FOR 1368 to R.S.U., K.S.O. and D.N.M.). K.S.O. is supported by the Urological Research Foundation.

DISCLOSURES

None.

REFERENCES

- Mehta RL, Cerdá J, Burdmann EA, Tonelli M, García-García G, Jha V, Susantitaphong P, Rocco M, Vanholder R, Sever MS, Cruz D, Jaber B, Lameire NH, Lombardi R, Lewington A, Feehally J, Finkelstein F, Levin N, Pannu N, Thomas B, Aronoff-Spencer E, Remuzzi G: International Society of Nephrology's Oby25 initiative for acute kidney injury (zero preventable deaths by 2025): A human rights case for nephrology. *Lancet* 385: 2616–2643, 2015
- Bellomo R, Kellum JA, Ronco C: Acute kidney injury. *Lancet* 380: 756–766, 2012
- Glodowski SD, Wagener G: New insights into the mechanisms of acute kidney injury in the intensive care unit. *J Clin Anesth* 27: 175–180, 2015
- Ghosh S, Hayden MS: Celebrating 25 years of NF- κ B research. *Immunol Rev* 246: 5–13, 2012
- Hinz M, Arslan SC, Scheidereit C: It takes two to tango: I κ Bs, the multifunctional partners of NF- κ B. *Immunol Rev* 246: 59–76, 2012
- Natoli G: NF- κ B and chromatin: Ten years on the path from basic mechanisms to candidate drugs. *Immunol Rev* 246: 183–192, 2012
- Guijarro C, Egido J: Transcription factor-kappa B (NF-kappa B) and renal disease. *Kidney Int* 59: 415–424, 2001
- Vos IH, Govers R, Gröne HJ, Kleij L, Schurink M, De Weger RA, Goldschmeding R, Rabelink TJ: NFkappaB decoy oligodeoxynucleotides reduce monocyte infiltration in renal allografts. *FASEB J* 14: 815–822, 2000
- Cao CC, Ding XQ, Ou ZL, Liu CF, Li P, Wang L, Zhu CF: In vivo transfection of NF-kappaB decoy oligodeoxynucleotides attenuate renal ischemia/reperfusion injury in rats. *Kidney Int* 65: 834–845, 2004
- Feng B, Chen G, Zheng X, Sun H, Zhang X, Zhang ZX, Xiang Y, Ichim TE, Garcia B, Luke P, Jevnikar AM, Min WP: Small interfering RNA targeting RelB protects against renal ischemia-reperfusion injury. *Transplantation* 87: 1283–1289, 2009
- Wan X, Fan L, Hu B, Yang J, Li X, Chen X, Cao C: Small interfering RNA targeting IKK β prevents renal ischemia-reperfusion injury in rats. *Am J Physiol Renal Physiol* 300: F857–F863, 2011
- Wullaert A, Bonnet MC, Pasparakis M: NF- κ B in the regulation of epithelial homeostasis and inflammation. *Cell Res* 21: 146–158, 2011
- Lentsch AB: Activation and function of hepatocyte NF-kappaB in postischemic liver injury. *Hepatology* 42: 216–218, 2005
- Neurath MF, Pettersson S, Meyer zum Büschenfelde KH, Strober W: Local administration of antisense phosphorothioate oligonucleotides to the p65 subunit of NF-kappa B abrogates established experimental colitis in mice. *Nat Med* 2: 998–1004, 1996
- Shibata W, Maeda S, Hikiba Y, Yanai A, Ohmae T, Sakamoto K, Nakagawa H, Ogura K, Omata M: Cutting edge: The I κ B kinase (IKK) inhibitor, NEMO-binding domain peptide, blocks inflammatory injury in murine colitis. *J Immunol* 179: 2681–2685, 2007
- Nenci A, Becker C, Wullaert A, Gareus R, van Loo G, Danese S, Huth M, Nikolaev A, Neufert C, Madison B, Gumucio D, Neurath MF, Pasparakis M: Epithelial NEMO links innate immunity to chronic intestinal inflammation. *Nature* 446: 557–561, 2007
- van Hogerlinden M, Rozell BL, Ahrlund-Richter L, Toftgård R: Squamous cell carcinomas and increased apoptosis in skin with inhibited Rel/nuclear factor-kappaB signaling. *Cancer Res* 59: 3299–3303, 1999
- Soriano P: Generalized lacZ expression with the ROSA26 Cre reporter strain. *Nat Genet* 21: 70–71, 1999
- Schmidt-Ullrich R, Aebischer T, Hülsken J, Birchmeier W, Klemm U, Scheidereit C: Requirement of NF-kappaB/Rel for the development of hair follicles and other epidermal appendages. *Development* 128: 3843–3853, 2001
- Bonventre JV, Yang L: Cellular pathophysiology of ischemic acute kidney injury. *J Clin Invest* 121: 4210–4221, 2011
- Daemen MA, van 't Veer C, Denecker G, Heemskerk VH, Wolfs TG, Clauss M, Vandenabeele P, Buurman WA: Inhibition of apoptosis induced by ischemia-reperfusion prevents inflammation. *J Clin Invest* 104: 541–549, 1999
- Beg AA, Sha WC, Bronson RT, Ghosh S, Baltimore D: Embryonic lethality and liver degeneration in mice lacking the RelA component of NF-kappa B. *Nature* 376: 167–170, 1995
- Subramanian A, Tamayo P, Mootha VK, Mukherjee S, Ebert BL, Gillette MA, Paulovich A, Pomeroy SL, Golub TR, Lander ES, Mesirov JP: Gene set enrichment analysis: A knowledge-based approach for interpreting genome-wide expression profiles. *Proc Natl Acad Sci U S A* 102: 15545–15550, 2005
- Dessing MC, Tammaro A, Pulsken WP, Teske GJ, Butter LM, Claessen N, van Eijk M, van der Poll T, Vogt T, Roth J, Florquin S, Leemans JC: The calcium-binding protein complex S100A8/A9 has a crucial role in controlling macrophage-mediated renal repair following ischemia/reperfusion. *Kidney Int* 87: 85–94, 2015
- Henke N, Schmidt-Ullrich R, Dechend R, Park JK, Qadri F, Wellner M, Obst M, Gross V, Dietz R, Luft FC, Scheidereit C, Müller DN: Vascular endothelial cell-specific NF-kappaB suppression attenuates hypertension-induced renal damage. *Circ Res* 101: 268–276, 2007

26. Höcherl K, Schmidt C, Kurt B, Bucher M: Inhibition of NF-kappaB ameliorates sepsis-induced downregulation of aquaporin-2/V2 receptor expression and acute renal failure in vivo. *Am J Physiol Renal Physiol* 298: F196–F204, 2010
27. Kinsey GR, Li L, Okusa MD: Inflammation in acute kidney injury. *Nephron, Exp Nephrol* 109: e102–e107, 2008
28. Kinsey GR: Macrophage dynamics in AKI to CKD progression. *J Am Soc Nephrol* 25: 209–211, 2014
29. Kucharczak J, Simmons MJ, Fan Y, Gélinas C: To be, or not to be: NF-kappaB is the answer—role of Rel/NF-kappaB in the regulation of apoptosis. *Oncogene* 22: 8961–8982, 2003
30. Yu EZ, Li YY, Liu XH, Kagan E, McCarron RM: Antiapoptotic action of hypoxia-inducible factor-1 alpha in human endothelial cells. *Lab Invest* 84: 553–561, 2004
31. Cockman ME, Lancaster DE, Stolze IP, Hewitson KS, McDonough MA, Coleman ML, Coles CH, Yu X, Hay RT, Ley SC, Pugh CW, Oldham NJ, Masson N, Schofield CJ, Ratcliffe PJ: Posttranslational hydroxylation of ankyrin repeats in IkappaB proteins by the hypoxia-inducible factor (HIF) asparaginyl hydroxylase, factor inhibiting HIF (FIH). *Proc Natl Acad Sci U S A* 103: 14767–14772, 2006
32. Bonventre JV, Zuk A: Ischemic acute renal failure: an inflammatory disease? *Kidney Int* 66: 480–485, 2004
33. Cugini D, Azzollini N, Gagliardini E, Cassis P, Bertini R, Colotta F, Noris M, Remuzzi G, Benigni A: Inhibition of the chemokine receptor CXCR2 prevents kidney graft function deterioration due to ischemia/reperfusion. *Kidney Int* 67: 1753–1761, 2005
34. Miura M, Fu X, Zhang QW, Remick DG, Fairchild RL: Neutralization of Gro alpha and macrophage inflammatory protein-2 attenuates renal ischemia/reperfusion injury. *Am J Pathol* 159: 2137–2145, 2001
35. Osborn L, Hession C, Tizard R, Vassallo C, Luhowskyj S, Chi-Rosso G, Lobb R: Direct expression cloning of vascular cell adhesion molecule 1, a cytokine-induced endothelial protein that binds to lymphocytes. *Cell* 59: 1203–1211, 1989
36. Sen R, Baltimore D: Inducibility of kappa immunoglobulin enhancer-binding protein NF-kappa B by a posttranslational mechanism. *Cell* 47: 921–928, 1986
37. Sanz AB, Sanchez-Niño MD, Ramos AM, Moreno JA, Santamaria B, Ruiz-Ortega M, Egido J, Ortiz A: NF-kappaB in renal inflammation. *J Am Soc Nephrol* 21: 1254–1262, 2010
38. Schmidt-Ullrich R, Mémet S, Lilienbaum A, Feuillard J, Raphaël M, Israel A: NF-kappaB activity in transgenic mice: developmental regulation and tissue specificity. *Development* 122: 2117–2128, 1996
39. Balogh A, Németh M, Koloszar I, Markó L, Przybyl L, Jinno K, Szigeti C, Heffer M, Gebhardt M, Szeberényi J, Müller DN, Sétáló G Jr, Pap M: Overexpression of CREB protein protects from tunicamycin-induced apoptosis in various rat cell types. *Apoptosis* 19: 1080–1098, 2014
40. Zhang JD, Patel MB, Griffiths R, Dolber PC, Ruiz P, Sparks MA, Stegbauer J, Jin H, Gomez JA, Buckley AF, Lefler WS, Chen D, Crowley SD: Type 1 angiotensin receptors on macrophages ameliorate IL-1 receptor-mediated kidney fibrosis. *J Clin Invest* 124: 2198–2203, 2014
41. Biju MP, Akai Y, Shrimanker N, Haase VH: Protection of HIF-1-deficient primary renal tubular epithelial cells from hypoxia-induced cell death is glucose dependent. *Am J Physiol Renal Physiol* 289: F1217–F1226, 2005

This article contains supplemental material online at <http://jasn.asnjournals.org/lookup/suppl/doi:10.1681/ASN.2015070748/-/DCSupplemental>.